METHANE PARTIAL OXIDATION BY THE LATTICE OXYGEN OF THE LANIO$_{3-\delta}$ PEROVSKITE. A PULSE STUDY

OXIDACIÓN PARCIAL DEL METANO USANDO EL OXÍGENO DE LA RED DE LA PEROVSKITA LANIO$_{3-\delta}$. ESTUDIO POR PULSOS

GERMÁN SIERRA GALLEGO
Escuela de Ingeniería de Materiales, Universidad Nacional de Colombia, Colombia, geasierraga@unal.edu.co

CATHERINE BATIOT-DUPEYRAT
Laboratoire de Catalyse en Chimie Organique, UMR CNRS 6503, Université de Poitiers, Ecole Supérieure d'Ingénieurs de Poitiers, catherine.batiot.dupeyrat@univ-poitiers.fr

FANOR MONDRAGÓN
Instituto de Química, Universidad de Antioquia,Colombia, fmondra@catios.udea.edu.co

Received for review July 23 th, 2009, accepted December 12 th, 2009, final version January, 3 th, 2010

ABSTRACT: $LaNiO_3$ perovskite was prepared by the self-combustion method and tested as catalyst for CH_4 activation using the oxygen lattice at 700°C and 800°C. Based on the non-stoichiometry experiments, the perovskite formula is written as $La^{3+}Ni^{3+}_{0.37}Ni^{2+}_{0.63}O_{2.68}$. When unreduced $LaNiO_{3-\delta}$ perovskite is used, only -type oxygen species were responsible for the partial CH_4 oxidation. Over non reduced perovskite high CH_4 conversions to H_2 and CO were obtained. CH_4 conversion and H_2, CO and CO_2, selectivities under quasi-stationary conditions were 100%, 80%, 98% and 2 % respectively at 800°C.
At the beginning of the reaction, a complete oxidation of methane to CO_2 and H_2O took place, whereas a partial oxidation to CO and H_2 was observed after that period. In such conditions the H_2/CO molar ratio obtained was 1.7, indicating a contribution of the parallel reverse water gas shift reaction

KEYWORDS: Methane partial oxidation; lattice oxygen; $LaNiO_{3-\delta}$ perovskite; auto combustion method

RESUMEN: La Perovskita $LaNiO_3$ fue preparada por el método de auto-combustión y probada como catalizador en la activación del CH_4 utilizando el oxígeno de la red a 700°C y 800°C. Basados en experimentos de no estequiometria se encontró que la fórmula de la perovskita es $La^{3+}Ni^{3+}_{0.37}Ni^{2+}_{0.63}O_{2.68}$. Cuando se usó la perovskita no reducida, solo las especies oxigeno β fueron las responsables de la oxidación parcial del CH_4. En este caso la conversión de CH_4 y las selectividades hacia H_2, CO y CO_2 en estado cuasi-estacionario fueron 100%, 80%, 98% y 2% respectivamente a 800°C.
Al principio de la reacción, la completa oxidación del metano hacia CO_2 y H_2O fue observada, mientras que la oxidación parcial hacia CO y H_2 fue la reacción predominante el resto de la reacción. La relación molar H_2/CO obtenida fue de 1.7, indicando la contribución de la reacción inversa de gas a agua en forma paralela.

PALABRAS CLAVE: Oxidación parcial del metano; oxígeno de la red; Perovskita $LaNiO_3$; Método de auto combustión

1. INTRODUCCIÓN

Syngas is an important feedstock for Fischer–Tropsch and methanol synthesis [1], as well as a precursor of hydrogen production. Most of the syngas is currently obtained from natural gas in which the main component is methane.

To date, a large-scale industrial route for syngas production comprises methane steam reforming (MSR), but an alternative technology is based on the catalytic partial oxidation of methane (POM):

$$CH_4 + \frac{1}{2}O_2 \rightarrow 2H_2 + CO \quad \Delta H°_{298} = -36 \text{ kJ/mol}$$

This process has some comparatively important differences with the well established steam reforming of methane. POM is mildly exothermic and does not require a high operating pressure and hence is more energy efficient [2-4]. The major drawback is related to the high costs of oxygen plants, and the use of dense ceramic membranes with mixed oxygen-ionic and electronic conductivity [5].

Many catalysts have been studied for the POM reaction. Most of them include non-noble (Ni, Co, Fe) and noble (Ru, Pt, Ir, Os, Rh, Pd) transition metals, usually deposited as fine particles over porous supports [6]. The production of synthesis gas by partial oxidation of CH_4 is also possible in using the SOFCs (solid oxide fuel cells).

$$CH_4 + O^{2-} \rightarrow CO + 2H_2 + 2e^- \quad Anode$$

$$\frac{1}{2}O_2 + 2e^- \rightarrow O^{2-} \quad Cathode$$

The oxidation technologies using SOFC-type reactors integrate oxygen separation and partial oxidation into a single step for methane conversion. Materials such as RuOx–ZrO_2 (8% mol Y_2O_3) composites [7], pyrochlore materials [8], ceria based materials [9] and perovskites [10] have been used as anodes or cathodes in solid oxide fuel cells (SOFCs).

A particularly attractive option for POM [11] and SOFCs [12-13] consists in the use of mixed metal oxide precursors with a perovskite structure, since these materials have also an exceptional high thermal stability. The general formula of these oxides is ABO_3, in which the cation A of a larger size is responsible for the thermal resistance of the catalyst whereas the cation B of smaller size accounts for the catalytic performance. Moreover, these oxides, due to their redox properties, are particularly attractive for the partial oxidation of methane [14].

Previous studies have shown that the particular behavior of the ABO_3 perovskites as oxidation catalysts is mainly due to the specific mobility of the lattice oxygen [15-16]. In this work, in the presence of $LaNiO_3$ perovskite the partial oxidation of methane was studied using only lattice oxygen species instead of gaseous oxygen. It was evidenced that oxygen from the lattice selectively oxidized methane with production of syngas

2. EXPERIMENTAL

2.1 Catalyst preparation

The $LaNiO_3$ perovskite was prepared by the self combustion method [17]. In the synthesis, $La(NO_3)_3 \cdot 6H_2O$ (Rhodia), $Ni(NO_3)_2 \cdot 6H_2O$ (Aldrich) and glycine (Merck) were used. All reagents were of analytical grade. Glycine ($H_2NCH_2CO_2H$) used as ignition promoter was added to an aqueous solution of metal nitrates with the appropriate stoichiometry, in order to get a $NO_3^-/NH_2 = 1$ ratio.

The resulting solution was slowly evaporated until a green gel was obtained. The gel was heated up to 250 °C at which the ignition reaction occured yielding a powdered precursor which still contained carbon residues. After calcination at 700°C for 8 hours all of the remaining carbon species were eliminated leading to the formation of the perovskite structure.

2.2 Characterization

The catalysts were characterized before and after the catalytic test by powder X-ray diffraction (XRD) using a Siemens D-5000 diffractometer with $CuK_{\alpha 1}$ = 1.5406 and $CuK_{\alpha 2}$ =1.5439 Å, operated at 40 kV and 40 mA. The diffraction patterns were recorded in the 2θ range 10-90° with a step of 0 .016° and 4s per step. Transmission and scanning electron microscopy were carried out on a Philips CM120 instrument, with a LaB_6 filament and equipped with an energy dispersive X-ray analyzer (EDX). The catalyst powder was first dispersed in *iso-*

propanol after grinding in an agate mortar and thereafter put on Cu grids for TEM observation. The specific surface area was obtained from the adsorption – desorption isotherm of N_2 using 30 % N_2/Ar as the adsorbate in a Micromeritics Flowsorb II 2300 apparatus at –196 °C. All samples were degassed for 30 minutes at 300°C before measurement.

Nonstoichiometric oxygen was experimentally determined by a thermogravimetric method [18-19], using a 2950 TA instrument microbalance. In the transient TGA experiments, 15 mg of the perovskite was put on the sample pan. Then the sample was heated up from room temperature to the desired temperature at a rate of 20 °C/min under a flow of pure O_2 at 1 atm. After the sample weighted reaches a steady-state value, the gas in the furnace was switched to helium.

Pulse experiments using a CH_4 flow were carried out in a quartz reactor (i.d. = 6 mm) at 700 °C and 800 °C under atmospheric pressure. Prior to each reaction, 50 mg of the powder catalyst was loaded into the reactor and preheated at 500 °C under 30 ml/min flow of He/O_2 (0.1% of oxygen) for 30 min in order to remove residual gases. Then, the reactor was cooled down to room temperature and the catalyst exposed to CH_4 pulses while the temperature of the reactor was increased from room temperature to 700 °C or 800 °C. The amount of gas in each pulse was 7.7 μmol, and the time interval between pulses varied from 1 min to 15 min. Between every CH_4 pulse, a flow of He/O_2 (0.1% of oxygen) used as carrier gas passed through the catalyst bed. The products of CH_4 conversion were analyzed on-line with a mass spectrometer. The same type experiment was performed using a reduced perovskite catalyst.

3.RESULTS AND DISCUSSION

3.1 Sample characterization

XRD patterns of the perovskite $LaNiO_3$ after calcination and after reduction are shown in Figure 1.

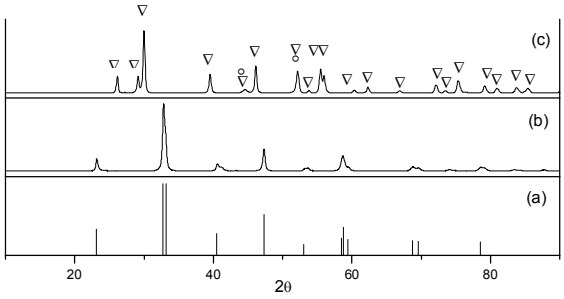

Figure 1. XRD patterns of the $LaNiO_3$ (a) JCPDF Card No. 330711, (b) after calcination at 700°C (c) and after reduction treatment. (°) Ni°, (∇) La_2O_3

After calcination at 700 °C only $LaNiO_3$ perovskite structure (Figure 1b) was observed. The diffraction lines are representative of the $LaNiO_3$ rhombohedral phase (JCPDF Card No. 33-0711- Figure 1a). After reduction treatment under hydrogen at 700°C, the $LaNiO_3$ perovskite structure was completely transformed into Ni° and La_2O_3 (Figure1c), which are the only phases observed.

3.2 Characterization by electron microscopy

SEM analysis was carried out after the perovskite calcination at 700°C and TEM characterization was done after the reduction treatment with H_2. The micrograph presented in the Figure 2a shows that the auto combustion method leads to the formation of a porous $LaNiO_3$ with a sponge appearance. TEM micrograph obtained after reduction of $LaNiO_3$ under hydrogen at 700 °C clearly shows the presence of spherical particles of nickel (Figure 2b). Based on the TEM micrograph, the average size of metallic particles was calculated using the following equation:

$$d = \sum_i n_i d_i^3 \,/\, \sum_i n_i d_i^2$$

Where n_i is the particle number and d_i is the characteristic diameter of particles [20].

The particle size distribution is reported in Figure 3, the particle size ranged between 2 and 50 nm and the average size of metallic particles was around 15 nm.

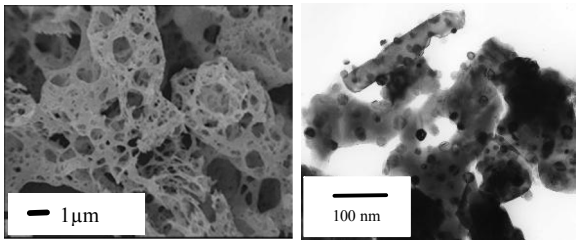

Figure 2. (a) SEM micrograph of $LaNiO_{3-\delta}$ after calcination and (b) TEM micrograph obtained after reduction of $LaNiO_{3-\delta}$ under hydrogen at 700°C

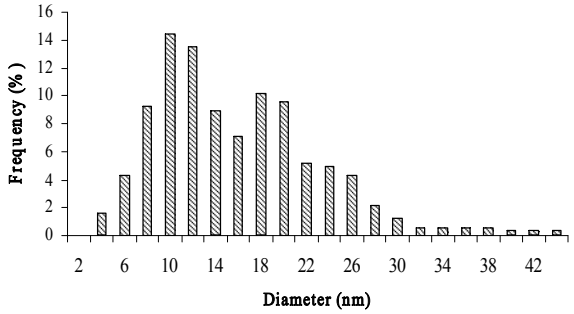

Figure 3. Ni Particle size distribution determined from TEM micrographs of $LaNiO_3$ reduced under hydrogen at 700°C

3.3 Characterization of oxygen non stoichiometric by thermo-gravimetric analysis

Figure 4 shows the weight changes after modification of the carrier gas (cycles $N_2 \rightarrow O_2$) at 800°C as follows: under nitrogen flow (curves a-b and c-d) and under oxygen flow (curves b-c and d-e). The initial mass loss under the nitrogen flow corresponds to desorption of water and carbon dioxide. When the carrier gas is switched from oxygen to nitrogen at 800 °C the weight of the $LaNiO_{3-\delta}$ sample decreases with time on stream as shown in Figure 4. Weight of the sample is restored if nitrogen is replaced by oxygen. The rate of the weight change is slower in the oxygen desorption period (curve c-d), than in the absorption period (curve d-e).

These results mean that a part of lattice oxygen can be removed from the sample at 800°C.

The overall oxygen content and the average Ni oxidation state were determined using the thermo-gravimetric analysis data. Thus, in the formula $LaNiO_{3-\delta}$ δ value is estimated to be 0.32 (in our experimental conditions), so that the perovskite formula can be rewritten as $LaNiO_{2.68}$.

This result is quite important because it shows that in $LaNiO_{2.68}$ perovskite about 63 % of the nickel in the structure correspond to Ni^{2+} species with the formation of oxygen vacancies, while about 37 % of the Ni remains as Ni^{3+}. Thus the perovskite formula is $La^{3+}Ni^{3+}_{0.37}Ni^{2+}_{0.63}O_{2.68}$.

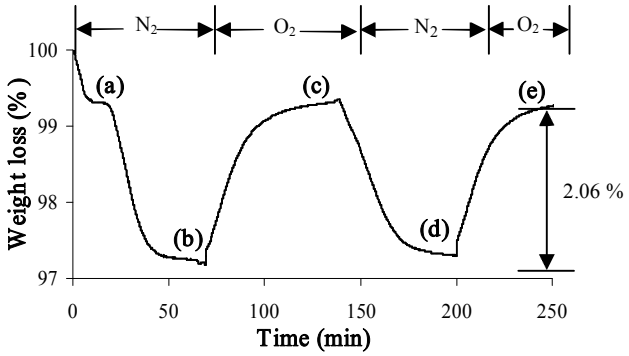

Figure 4. Weight change of $LaNiO_{3-\delta}$ during nitrogen→oxygen→nitrogen→oxygen cycles at 800°C

In several previous publications, it was also reported that the decomposition of $LaNiO_3$ to produce the structures La_2NiO_4 or $La_4Ni_3O_{10}$ and NiO occurred at elevated temperatures between 800 and 1100 °C in both air and inert gases [21-22]. To verify if the perovskite structure was maintained during the nitrogen→oxygen→nitrogen→oxygen cycles at 900°C, an *in-situ* XRD analysis was performed (See Figure 5).

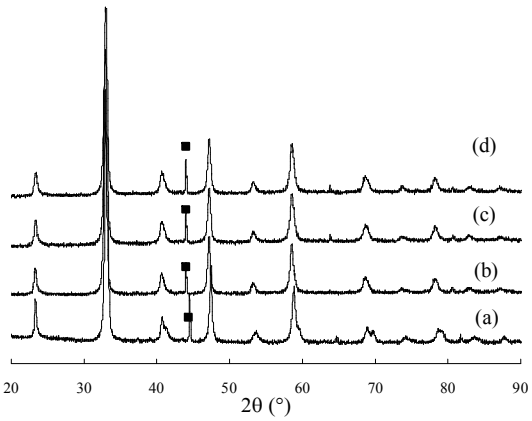

Figure 5. DRX of $LaNiO_3$ during nitrogen→oxygen→nitrogen→oxygen cycles. (a) at room temperature, (b) at 900 °C over oxygen, (c) at 900 °C over nitrogen and (d) at 900 °C over oxygen. (■) sample holder

It can be observed (Figure 5) that during the oxygen adsorption and desorption steps the perovskite structure remains unchanged showing a high stability in these conditions or perhaps a rather low phase transformation (with a slow kinetics to be observed), which could explain the reversibility of the process as shown in Figure 4.

3.4 Reactivity of lattice oxygen in the oxidation of methane

The partial oxidation of methane by pulsed reaction over the $LaNiO_{3-\delta}$ catalysts was studied at 700 °C and 800 °C. First, a blank experiment was carried out without catalyst under usual experimental conditions in order to evidence the thermal decomposition of methane. In all cases the CH_4 conversion was lower than 1%. Then, methane pulses were introduced each 15 minutes over the non reduced $LaNiO_{3-\delta}$ perovskite, in order to examine the reactivity of lattice oxygen (between pulses, carrier gas He/O_2 (0.1% O_2) was continuously flowed through the catalyst bed).

At 700°C there was no catalytic activity and CH_4 conversion remained equal to 1%. At 800 °C the results are displayed in the Figure 6. The only products detected were H_2, CO, and CO_2, which indicates that methane is effectively oxidized by the lattice oxygen of the perovskite oxide (the amount of water produced in the reaction was not quantified). Figure 6 also shows that CO and H_2 productions begin almost at the same time when the CO_2 production goes through a maximum before declining (pulse 18). The decline in the CO_2 production suggests a decrease of the concentration of surface active oxygen species.

After 25 pulses the amount of H_2 and CO indicates that the partial oxidation (POM) of methane is taking place at a significant extent with a very high selectivity. At this point it is possible that the hydrogen reduces the catalyst so that Ni° particles are available as active sites for the methane activation. Then it is suggested that carbon species can be formed over the metal active sites from the dissociation of methane and further completely oxidized to synthesis gas by the oxygen lattice. Under steady conditions the CH_4 conversion is 100% and the CO_2, CO and H_2 selectivities are 2, 98 and 80 % respectively without formation of carbon deposits at the catalyst surface.

The perpendicular dotted line represents the pulse number when the temperature of the reactor reached 800 °C.

It is expected that if the reaction followed the stoichiometry of the POM, the CO and H_2 selectivities should be similar, with a H_2/CO molar ratio equal to 2. In our case, the selectivity to H_2 is lower giving a H_2/CO molar ratio of 1.7. This result suggest that there is a contribution of the reverse water gas shift reaction.

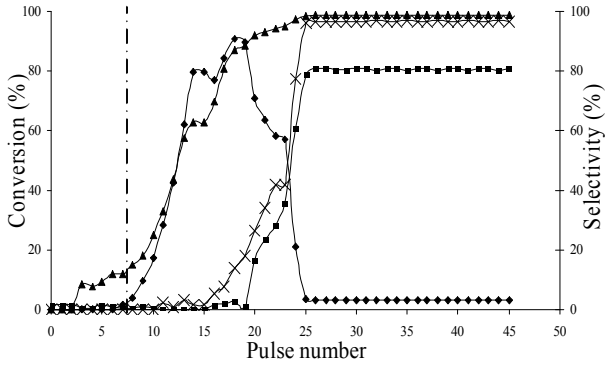

Figure 6. Methane pulsed oxidation reaction (7.7 μmol/pulse) over non reduced $LaNiO_{3-\delta}$ perovskite at 800 °C. A pulse was injected every 15 min. (▲) CH_4, (♦) CO_2, (×) CO and (■) H_2

From the comparison of the results of pulsed experiments at 700 ºC and 800 °C, it is evident that β-type oxygen species (atomic oxygen originating from the bulk which desorbs at high temperatures) are the only oxygen species responsible for the partial oxidation reaction. Thus, it is clear that the bulk lattice oxygen of $LaNiO_{3-\delta}$ perovskite should participate in the partial oxidation of CH_4 to H_2 and CO. The TGA experiments (Figure 4) show that there are non stoichiometric oxygen and oxygen vacancies involved in the oxygen transport through the lattice [23]. In a recent publication it was found that the selectivity towards the total and partial oxidation of methane using $La_{0.3}Sr_{0.7}Fe_{0.8}M_{0.2}O_{3-\delta}$ (M= Ga, Al) perovskites, was related to the amount of nonstoichiometric

oxygen [24]. The relationship between the rate of oxygen migration and the concentration of oxygen vacancies was also confirmed by Rossetti *et al* [25].

A complementary experiment using the pulse technique was conducted at 800°C in order to study the behavior of the lattice oxygen during a quasi-continuous operating reaction. The results are displayed in the Figure 7. The experiments can be described as follows:

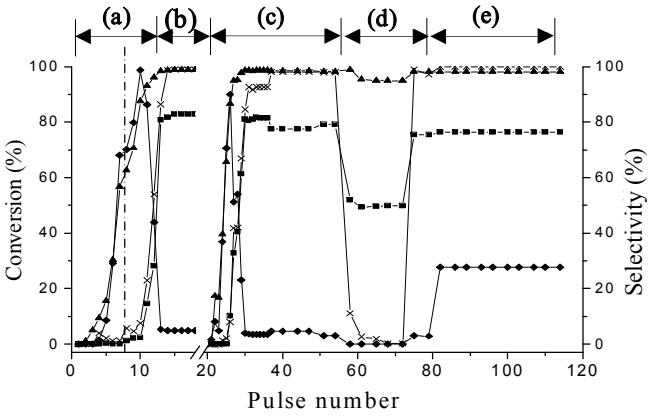

Figure 7. Methane pulsed oxidation reaction (7.7 μmol/pulse) over non reduced $LaNiO_{3-\delta}$ perovskite at 800 °C. Pulse composition: (a) CH_4 (every 15 min), (b) O_2/He - 5% of oxygen (every 15min), (c) CH_4 (every 15 min), (d) CH_4 (every 1min) and (e) CH_4 (every 15 min). (▲) CH_4, (♦) CO_2, (×) CO, (■) H_2

In the first part (segment (*a)* of Figure 7), the pulse sequence is the same as the one described above. Pulses of methane were injected each 15 min, while the temperature was increased from room temperature to 800 °C. After that, a higher oxygen concentration was used (He/O_2 - 5% of oxygen) during 30 min, with the aim of re-oxidizing the sample and refill the maximum number of the oxygen vacancies, (segment (*b)* in the Figure 7). Then 30 pulses of methane were injected again at intervals of 15 min using He/O_2 (0.1% of oxygen) as carrier gas (segment (*c)* of the Figure 7. In order to approach a continuous operation and to determine how fast the catalyst can recover the oxidation capability, pulses of CH_4 were injected at intervals of 1 min, (segment (*d)* Figure 7). Finally, the pulses frequency was reduced to every 15 min (segment (*e)* Figure 7*)*. The carbon balance of all these experiments is reported in the Figure 8. The selectivities and conversion profiles shown in Figure 7 are similar to those presented in the Figure 6. Comparison of segments (*a*) and (*c*) shows that re-oxidation process of the catalyst is reversible, and that the oxygen vacancies can be easily regenerated. Under steady conditions CH_4 conversion and CO_2, CO and H_2 selectivities are the same as those obtained at 700°C (Figure 6).

Methane conversions as well as CO and H_2 selectivities were constant during 25 pulses, segment (*c*). At the same time, carbon balance (not shown) revealed that there was not carbon deposition on the catalyst surface during the pulsed experiments. This result suggests that partial oxidation is the main reaction taking place and that the catalytic methane pyrolysis, if any, is a minor reaction.

The perpendicular dotted line represents the pulse number when the temperature of the reactor reached 800 °C.
The results show that the oxygen required in the partial oxidation is i) extracted from the $LaNiO_{3-\delta}$ lattice during the CH_4 pulses and ii) regenerated by direct activation of molecular oxygen contained in the carrier gas.

Indeed if the time between pulses was reduced from 15 min to 1min, segment (*d*), CH_4 dissociation was observed and carbon deposition took place on the $LaNiO_{3-\delta}$ perovskite surface due to a lower surface concentration of oxygen species close to the carbon species deposited on the active sites which could also indicate a limited oxygen mobility. During these 20 consecutives CH_4 pulses in segment (*d*), only H_2 was formed and CO selectivity decreased towards zero. Here, carbon deposits were detected, indicating that pyrolysis of CH_4 takes place (Figure 8).

After re-increasing the pulse intervals to 15 min (segment (*e*)), CO was produced again and a large amount of CO_2 was also detected. The carbon balance is considerably lowered due to the oxidation of the carbonaceous deposits over the catalyst surface, which originated from the

previous methane dissociation (segment (*e*) in the Figure 8).

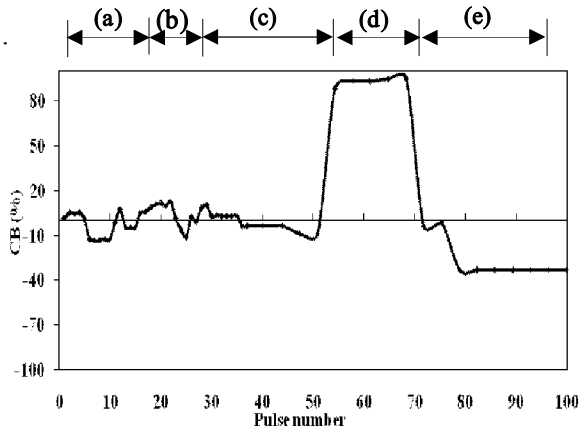

Figure 8. Carbon balance for the methane pulses series of the Figure 7

3.5 Methane partial oxidation mechanism over the $LaNiO_{3-\delta}$ perovskite

Taking into account the above observations and the results published in the literature, the following mechanism is suggested.
First, it is necessary to consider the oxygen incorporation into the lattice. This process has been studied using isotopic oxygen exchange with different oxides. It is generally accepted that O_2 incorporation into the lattice occurred as follows, [26].

$$O_2 + e' \leftrightarrow O_2^-$$
$$O_2^- + e' \leftrightarrow O_2^{2-}$$
$$O_2^{2-} \leftrightarrow 2O^-$$

Several species can appear as intermediates in the reduction of molecular oxygen, such as O_2^-, O_2^{2-}, and O^-. In this work we did not attempt to distinguish between these three surface oxygen species, and therefore they are denoted as O*. The Kröger-Vink notation is used for lattice defects [27]: $V_o^{\cdot\cdot}$ denotes an oxygen vacancy, $O_O^{\times}$ a regular lattice oxygen ion, and e' an electron. The subscripts s and b refer to "surface" and "bulk," respectively. This distinction is necessary because only the surface lattice oxygen will be accessible for the catalytic reaction. The same argument also holds for oxygen vacancies.

In the first part of the reaction, when there is a high concentration of reactive lattice oxygen, CH_4 is completely oxidized to form CO_2 and H_2O.

$$CH_4 + 4O_O^X \rightarrow CO_2 + 2H_2O + 4V_O^{\cdot\cdot}$$

or

$$CH_4 + 4O^* \rightarrow CO_2 + 2H_2O$$

A low concentration of extractible lattice oxygen favors selective oxidation of methane to CO and H_2, and the reaction mechanism can be expressed as:

$CH_4 \rightarrow CH_{4-x} + x\ H_S$
$CH_{4-x} \rightarrow C_s + (4-x)\ H_S$
$H_S + H_S \rightarrow H_{2,S} \rightarrow H_{2,g}$
$C_S + O^* \rightarrow CO_s$
$CO_s \rightarrow CO_g$
$CO + O^* \rightarrow CO_{2,s}$
$CO_{2,s} \rightarrow CO_{2,g}$
$2H_S + O^* \rightarrow H_2O_S$
$H_2O_S \rightarrow H_2O_g$

The methane molecule can be also dissociated by the oxygen species according to the following equation [28]:

$CH_{4,S} + O^* \rightarrow CH_{3,S} + OH_S$
$CH_{3,S} + 3O^* \rightarrow C_s + 3OH_S$

In this step, the adsorbed H atom may combine to form hydrogen which easily desorbs. The chemisorbed carbon species are either oxidized to CO by lattice oxygen or oxidized to CO_2.
According to the above scheme, the product distribution of the POM reaction over $LaNiO_{3-\delta}$ catalyst was determined by the concentration of surface oxygen species, which is affected by the migration rate of oxygen from the bulk toward the surface.

Finally, the re-oxidation process can be written as function of an incorporation and migration process:

$$O^- + V_{O,s}^{\cdot\cdot} + e' \leftrightarrow O_{O,s}^X \qquad \textit{Incorporation}$$
$$O_{O,s}^X + V_{O,b}^{\cdot\cdot} \leftrightarrow O_{O,b}^X + V_{O,s}^{\cdot\cdot} \qquad \textit{Migration}$$

According to our results, these vacancies can be re-filled with oxygen either by direct activation of oxygen from the gas phase or by lattice oxygen diffusion. Lattice oxygen diffusion may provide an alternative pathway for replenishment of the surface lattice oxygen consumed by methane. This may explain the high methane conversion over the $LaNiO_3$ catalyst.

4. CONCLUSIONS

The perovskite $LaNiO_3$ prepared by the auto combustion method has a nonstoichiometric oxygen and that its formula can be rewritten as $La^{3+}Ni^{3+}_{0.368}Ni^{2+}_{0.632}O_{2.684}$.

Perovskite oxygen lattice has catalytic activity towards CH_4 partial oxidation at 800 °C while at a lower temperature the conversion is negligible. Complete oxidation of methane to CO_2 and H_2O occurs during the first step of the reaction (initial pulses), whereas partial oxidation to CO and H_2 is found to be the main reaction during the subsequent pulses. A high concentration of available lattice oxygen promotes total oxidation of CH_4 to CO_2 and H_2O, while a low concentration of lattice oxygen favors selective oxidation of methane to CO and H_2. High methane conversions and large amounts of H_2 and CO were produced using non reduced perovskite, with a CH_4 conversion and H_2, CO and CO_2, selectivities under steady conditions of 100%, 80%, 98% and 2 % respectively at 800°C. The H_2/CO ratio obtained was 1.7, indicating a contribution of the reverse water gas shift reaction

5. ACKNOWLEDGEMENTS

The authors are grateful to the PICS program: "Valorization of natural gas and Fischer-Tropsch synthesis" for the financial support given. F. Mondragon and G. Sierra acknowledge to the University of Antioquia for the financial support of the Sostenibilidad Program and to Colciencias for the support of the project 1115-06-17639. G. Sierra thanks COLCIENCIAS and the University of Antioquia for the PhD scholarship.

REFERENCES

[1] YORK, A.P.E., XIAO, T. GREEN, M.L.H. Brief Overview of the Partial Oxidation of Methane to. Synthesis Gas, Top. Catal., 22, 345-358, 2003.

[2] DISKIN, A.M., ORMEROD, R.M. Partial Oxidation of Methane over. Supported Nickel Catalysts, Stud. Surf. Sci. Catal., 130, 3519 –3524, 2000.

[3] LIU, Z.W. JUN, K.W. ROH, H.S. PARK, S.E. OH, Y.S. Partial Oxidation of Methane over Nickel Catalysts Supported on Various Aluminas, Korean J. Chem. Eng., 19, 735-735, 2002.

[4] CHEN, Y. HU, C. GONG, M. CHEN, Y. TIAN, A. Partial oxidation and chemisorption of methane over Ni/Al_2O_3 catalysts, Stud. Surf. Sci. Catal. 130, 3543-3548, 2000.

[5] MAZANEC, T.J. PRASAD, R. ODEGARD, STEYN, R. C. ROBINSON, E.T. Oxygen transport membranes for syngas production, Stud. Surf. Sci. Catal. 136. 147-152, 2001.

[6] LAGO, R. BINI, G. PEÑA, M.A FIERRO, J.L.G. Partial Oxidation of Methane to Synthesis Gas Using $LnCoO_3$ Perovskites as Catalyst Precursors, J. Catal. 167, 198-209, 1997.

[7] BEBELIS, S. NEOPHYTIDES, S. KOTSIONOPOULOS, N. RIANTAFYLLOPOULOS, N. COLOMER, M.T. JURADO, J. Methane oxidation on composite ruthenium electrodes in YSZ cells, Solid State Ionics. 177, 2087-2091, 2006.

[8] KUMAR, M. ANBU KULANDAINATHAN, M. ARUL RAJ, I. CHANDRASEKARAN, R. PATTABIRAMAN, R. Electrical and sintering behaviour of $Y_2Zr_2O_7$ (YZ) pyrochlore based materials: the influence of bismuth, Mater. Chem. Phys. 92 303-309, 2005.

[9] KHARTON, V.V. YAREMCHENKO, A.A. VALENTE, A.A. FROLOVA, E.V IVANOVSKAYA, M.I. FRADE, J.R. MARQUES, F.M.B. ROCHA, J. Methane oxidation over SOFC anodes with nanocrystalline ceria-based phases, Solid State Ionics, 177, 2179-2183, 2006.

[10] SUN, X.F. GUO, R.S. LI, J. Preparation and properties of yttrium-doped $SrTiO_3$ anode materials, Ceramics International. 34, 219-223, 2008.

[11] LABHSETWAR, N.K. WATANABE, A. MITSUHASHI, T. New improved syntheses of $LaRuO_3$ perovskites and their applications in environmental catalysis. Catal. B: Environ., 40 21-30, 2003.

[12] SAUVET, A.L. FOULETIER, J. GAILLARD, F. PRIMET, M. Surface Properties and Physicochemical Characterizations of a New Type of Anode Material, $La_{1-x}Sr_xCr_{1-y}Ru_yO_{3-\delta}$, for a Solid Oxide Fuel Cell under Methane at Intermediate Temperature, J. Catal., 209, 25-34, 2002.

[13] HWANG, H.J. MOON, J.W. LEE, S. LEE, E.A. Electrochemical performance of LSCF-based composite cathodes for intermediate temperature SOFCs, Journal of Power Sources, 145, 243-248, 2005.

[14] BARBERO, J. PEÑA, M.A. CAMPOS-MARTIN, J.M. FIERRO, J.L.G. ARIAS, P.L. Support effect in Ni-supported catalysts on their performance for methane partial oxidation, Catal. Lett., 87, 211-218, 2003.

[15] PEÑA, M.A., FIERRO, J.L.G. Chemical structures and performance of perovskites oxides, Chem. Rev. 101, 1981-2017, 2001.

[16] FALCÓN, H. BARBERO, J.A. ARAUJO, G. CASAIS, M.T. MARTINEZ-LOPEZ, M.J. ALONSO, J.A. FIERRO, J.L.G. Double perovskite oxides $A_2FeMoO_{6-\delta}$ (A=Ca, Sr and Ba) as catalysts for methane combustion, Appl. Catal. B: Environ., 53, 37-45, 2004.

[17] PECHINI, R. Method of preparing lead ans alkaline earth titanates and niobates and coating method using the same to form a capacitor,US Patent No 3,330,697 (1967).

[18] ZENG, Y., LIN, Y.S. A transient TGA study on oxygen permeation properties of perovskite-type ceramic membrane, Solid State Ionics, 110, 209-221, 1998.

[19] YANG, Z., LIN, Y.S. A semi-empirical equation for oxygen nonstoichiometry of perovskite-type ceramics, Solid State Ionics. 150, 245-254, 2002.

[20] MUSTARD, D.G. BARTHOLOMEW, C.H. Determination of metal crystallite size and morphology in supported nickel catalysts, J. Catal., 67, 186-206, 1981.

[21] ZINKEVICH, M., ALDINGER, F. Thermodynamic analysis of the ternary La-Ni-O system, J. Alloys and Compounds. 375, 147-161, 2004.

[22] MARTÍNEZ-LOPE, M.J. CASAIS, M.T. ALONSO., J. A., Stabilization of Ni^+ in defect perovskites $La(Ni_{1-x}Al_x)O_{2+x}$ with infinite-layer structure, Journal of Alloys and Compounds, 275, 109-112, 1998.

[23] RAMOS, T. ATKINSON, A. Oxygen diffusion and surface exchange in $La_{1-x}Sr_xFe_{0.8}Cr_{0.2}O_{3-\delta}$ (x=0.2, 0.4 and 0.6), Solid State Ionics. 170, 275-286, 2004.

[24] KHARTON, V.V., PATRAKEEV, M.V., WAERENBORGH, J.C., SOBYANIN, V.A., VENIAMINOV, S.A., YAREMCHENKO, A.A., GACZYŃSKI, P., BELYAEV, V.D., SEMIN, G.L., AND FRADE, J.R., Methane oxidation over perovskite-related ferrites: Effects of oxygen nonstoichiometry, Solid State Sciences. 7, 1344-1352, 2005.

[25] ROSSETTI, I. FORNI, L. Catalytic flameless combustion of methane over perovskites prepared by flame–hydrolysis, Appl. Catal. B. 33, 345-352, 2001.

[26] ZHU, J. VAN OMMEN, J.G. BOUWMEESTER, H.J.M. LEFFERTS, L. Activation of O_2 and CH_4 on yttrium-stabilized zirconia for the partial oxidation of methane to synthesis gas, J. Catal. 233, 434-441, 2005.

[27] Kroger, F.A. The Chemistry of Imperfect Crystals. Vol. 2. Imperfection Chemistry of Crystalline Solids. Elsevier, New York, 1974.

[28] AU, C.T. AND WANG, H.Y. Mechanistic Studies of Methane Partial Oxidation to Syngas over SiO_2-Supported Rhodium Catalysts, J. Catal. 167, 337-345, 1997.